Solubility enhancement in supercritical solvents

Benjamin C.-Y. Lu, Dingan Zhang and Wei Sheng

Department of Chemical Engineering, University of Ottawa, Ottawa, Ontario, Canada K1N 9B4

Abstract - The enhancement of solubility of a solid in a supercritical solvent is interpreted with emphasis placed on binary mixtures of the second class. The selection of supercritical solvent ; the choice of temperature and pressure for supercritical fluid extractions; the characteristics of solubility curves between and in the vicinities of the upper critical and the lower critical end points; the effects of density and density-dependent properties; and the addition of an entrainer and its chemical affinity on the solubility enhancement are discussed. The correlations using a cubic equation of state for solid solubilities in a solvent with or without a cosolvent are presented.

INTRODUCTION

A supercritical fluid (SCF) is one of which the temperature and pressure exceed its critical temperature T_c and pressure P_c. In the supercritical region, the density of a SCF is a continuous function of its pressure (or temperature) at a given temperature (or pressure). In the vicinity of the critical point, physical properties of the fluid are significantly transformed and the solubility of substances (solid or liquid) changes greatly as well. The separation process of supercritical fluid extraction (SFE) is a technique that utilizes the separation process of the solvent power of SCF at temperatures and pressures near its critical point. One of the attractive features of the SFE technology is that it is suitable for separation of high boiling components from mixtures as it is typically carried out at low or moderate temperatures. Energy saving is also possible in the solvent recovery. It has been used or is being developed as a separation process for the food processing, pharmaceutical, cosmetics and perfume, chemical and energy-related industries.

A SCF has a density comparable to liquid densities and therefore has the solvent power close to that of liquids. For example, carbon dioxide (T_c = 304.2 K, P_c = 73.8 bars) has a density of 7 x 10^2 kg/m^3 at 305 K and 139 bar. Observation of the solvent power of supercritical ethanol on solubility of potassium iodide was noted by Hannay and Hogarth (ref. 1) as early as in 1879. The solvent power of a SCF may vary over a wide range by varying temperature or pressure. In the region with $1.0 < T_r < 1.2$ and $P_r > 1$, supercritical fluids are highly compressible. A slight change in temperature and pressure would result in a considerable density change of the SCF. The recovery of the dissolved and entrained material can be manipulated by lowering the density of the SCF. There is still a need to have a better understanding of the solubility behavior which is closely related to solution chemistry and to develop models for correlating and predicting the enhancement of the solubility of solute in supercritical solvents.

SOLID–SCF PHASE EQUILIBRIA

The two types of solid-SCF phase diagrams for binary mixtures have been described previously (ref. 2). The triple point temperature of the solid under consideration is greater than the critical temperature of the fluid, and there is no common range of temperature in which both pure components are in the liquid state. Emphasis of this discussion is placed on the second class (Type II) of mixtures, which are of great interest in SFE operations. Unlike that for a Type I mixture, the critical mixture curve for a Type II mixture does not run continuously on a pressure-temperature (P - T) projection between the critical points of the two pure components as shown in Fig. 1. It is intersected twice by the three-phase solid-liquid-gas (S-L-G) curves. The two intersection points are called the lower critical end point (LCEP) which is found to be close to the critical point of the pure solvent and the upper critical end point (UCEP). The P-T projections for Type II mixtures may be further classified into three categories according to the shape of the higher temperature branch of the S-L-G curve as depicted in Fig. 1.

ISOTHERMAL SOLUBILITY CURVE

When an isothermal solubility curve of a solid in a SCF, such as naphthalene in ethylene (ref. 3), is plotted on a mole fraction of the solute in the fluid phase (y_2) versus pressure (P) diagram as shown in Fig. 2, the curve starts with a negative slope at low pressure (the solubility of solid decreases with pressure), passes through a minimum, and then the mole fraction increases with increasing pressure at high pressure (solubility enhancement). The minimum solubility is useful in the purification of the SCF solvent, such as the removal of the impurity carbon dioxide from air by cooling the high-pressure air and separating the solid dry-ice at an optimum pressure corresponding to the minimum solubility at a given temperature (ref. 4). But the application of SFE is more concerned with the extraction and recovery of solute.

Although it is not shown in Fig. 2, there is also a maximum solubility in solid-fluid equilibria. Concentration maxima have been reported by Czubryt et al. (ref. 5) in their solubility measurements of Carboway 4000, Carboway
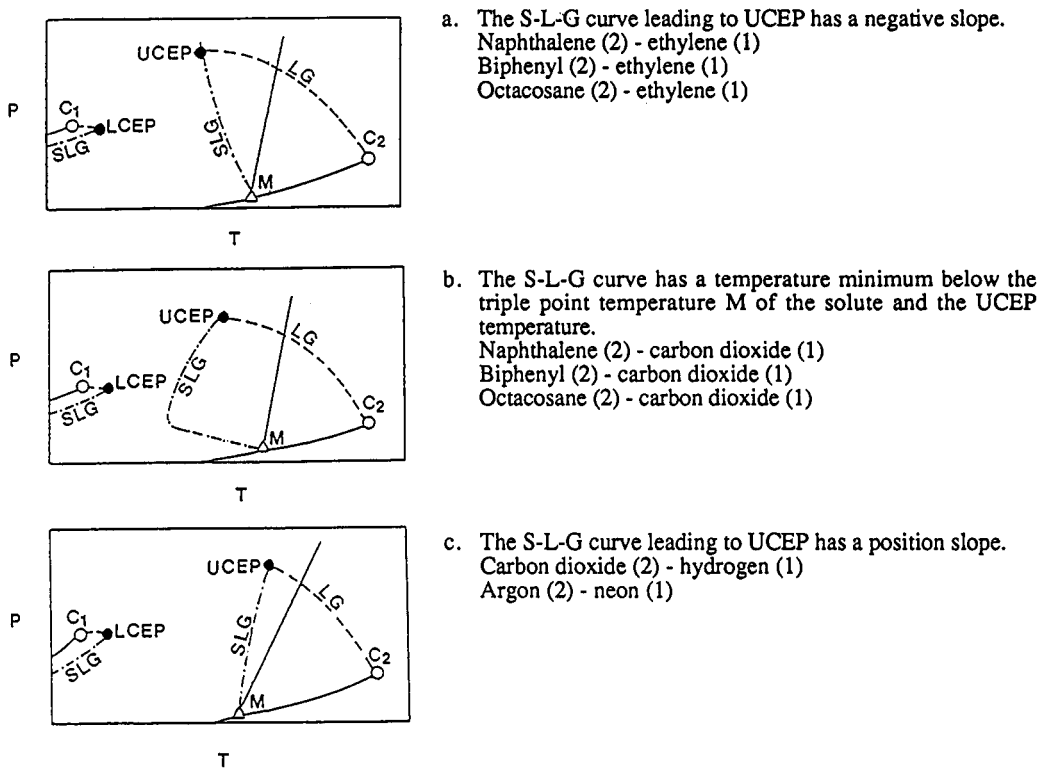
a. The S-L-G curve leading to UCEP has a negative slope.
    Naphthalene (2) - ethylene (1)
    Biphenyl (2) - ethylene (1)
    Octacosane (2) - ethylene (1)

b. The S-L-G curve has a temperature minimum below the
    triple point temperature M of the solute and the UCEP
    temperature.
    Naphthalene (2) - carbon dioxide (1)
    Biphenyl (2) - carbon dioxide (1)
    Octacosane (2) - carbon dioxide (1)

c. The S-L-G curve leading to UCEP has a position slope.
    Carbon dioxide (2) - hydrogen (1)
    Argon (2) - neon (1)

Fig. 1. Pressure-temperature projections for binary mixtures with a supercritical solvent (1) and a slightly volatile
solute (2). ---- L = G loci, - . - .- three phase S - L - G coexistence curve; C_1, C_2, critical points; M, triple point of
the solute.

100, 1-octadecanol and stearic acid in carbon dioxide at 313 K between 304 and 2533 bars. The maximum concen-
tration is of importance to SFE applications.

At equilibrium, the chemical potential of the solute in the solid phase μ_2^s is equal to that in the fluid phase μ_2^g,

$$\mu_2^s(T,P) = \mu_2^g(T,P,y_2) \tag{1}$$

With the assumption that the solubility of the solvent in the solid is negligible, isothermal changes of pressure along
the equilibrium line leads to

$$\left(\frac{\partial \mu_2^s}{\partial P}\right)_T dP = \left(\frac{\partial \mu_2^g}{\partial P}\right)_{T,y_2} dP + \left(\frac{\partial \mu_2^g}{\partial y_2}\right)_{T,P} dy_2 \tag{2}$$

Since $\left(\partial \mu_2^s / \partial P\right)_T = v_2^s$ and $\left(\partial \mu_2^g / \partial P\right)_{T,y_2} = \bar{v}_2^g$, we obtain

$$\left(\frac{\partial y_2}{\partial P}\right)_T = \frac{v_2^s - \bar{v}_2^g}{\left(\partial \mu_2^g / \partial y_2\right)_{T,P}} \tag{3}$$

where v_2^s is the molar volume of the solid solute and $\bar{v}_2^g$ is the partial molar volume of the solute in the fluid phase.
An alternative expression of eqn. (3) to facilitate the computation of the variation of y_2 with P is given by

$$\left(\frac{\partial \ln y_2}{\partial P}\right)_T = \frac{(v_2^s - \bar{v}_2^g)/RT}{\left[1 + \left(\partial \ln \hat{\phi}_2 / \partial \ln y_2\right)_{T,P}\right]} , \tag{4}$$

which may be obtained from $\hat{\phi}_2 = \hat{f}_2 / y_2 P$ and the definition of $\hat{f}_2$ in terms of μ_2^g (ref. 6),

$$\mu_2^g = \mu_2^o + RT \ln \hat{f}_2 \tag{5}$$

and

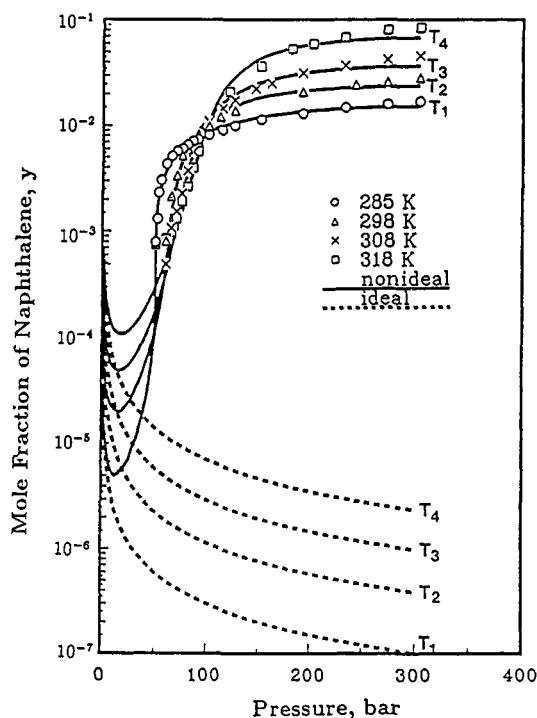$$\hat{f}_2 / p_2 \to 1 \text{ as } P \to 0 \tag{6}$$

Fig. 2. Measured and calculated solubility of naphthalene in ethylene (Data of ref. 3)

In these expressions, $\bar{p}_2$, $\hat{f}_2$, and $\hat{\phi}_2$ are the partial pressure, fugacity and fugacity coefficient of the solute in the fluid phase, respectively.

Kurnik and Reid (ref. 7) calculated the solubility minimum and maximum along an isothermal curve using the solubility of naphthalene in ethylene as an example system. They used the Peng-Robinson (PR) equation of state (ref. 8) to calculate $\hat{\phi}_2$ and $\bar{v}_2^g$ of eqn. (4). *The thermodynamic relationship between* $\hat{\phi}_2$ *and an equation of state is given by* (ref. 9)

$$RT \ln \hat{\phi}_2 = RT \ln \frac{\hat{f}_2}{y_2 P} = \int_v^\infty \left[\left(\frac{\partial P}{\partial n_2} \right)_{T,v,n_1} - \frac{RT}{v} \right] dv - RT \ln z \tag{7}$$

where z is the compressibility factor of the mixture. For a pressure-explicit equation of state, such as the PR equation, the most convenient procedure for calculating $\bar{v}_2$ is to use the exact relationship

$$\bar{v}_2 = - \left(\frac{\partial P}{\partial n_2} \right)_{T,V,n_1} \bigg/ \left(\frac{\partial P}{\partial V} \right)_{T,n_1,n_2} \tag{8}$$

They observed that $\left(\partial \ln \hat{\phi}_2 / \partial \ln y_2 \right)_{T,P}$ was never less than -0.4 over a pressure range up to the 4 k bar limit studied. The computed $\bar{v}_2^g$ for naphthalene in ethylene is large and positive at low pressures. It decreases with an increase in P and becomes equal to $v_2^{s\cdot}$ At this pressure, $\left(\partial \ln y_2 / \partial P \right)_T$ equals zero corresponding to the solubility minimum. Further increase of P makes $\bar{v}_2^g$ more negative and reaches a minimum, corresponding to the inflection point of the solubility curve. At high pressures, $\bar{v}_2^g$ increases and eventually becomes equal to v_2^s and $\left(\partial \ln y_2 / \partial P \right)_T = 0$ again, corresponding to the solubility maximum. The enhancement of solute solubility occurs between the two extrema. It is in this region, one would like to employ SFE processes.

SOLUBILITY ENHANCEMENT

In the consideration of solubility enhancement in supercritical solvents, a binary system considered above involving a solid solute and a SCF represents the simplest case. The assumption stated in the above section is adopted as in the conventional approach. The solubility of the solute in the SCF solvent, y_2, is given by

$$y_2 = E(p_2^{sat}/P) \tag{9}$$

where E is the enhancement factor, representing the solubility increase in the supercritical solvent over that in an ideal gas mixture, p_2^{sat} is the vapor pressure (sublimation pressure) of the pure solid and P is the system pressure. For the so-called ideal solubility, E equals unity. The ideal solubility curves are shown in Fig. 2 by the dashed lines for comparison.

Determination of E from $\hat{\phi}_2$

An empirical equation of state, such as the PR equation mentioned above, may be used to evaluate E by equating the fugacities of the solute in the solid phase and in the fluid (gas) phase. Using the same assumption mentioned above and taking v_2^s to be pressure independent, the following expression of E is obtained:

$$E = \left(\phi_2^{s}/\hat{\phi}_2\right) \exp\left[v_2^s \left(P - p_2^{sat}\right)/RT\right] \tag{10}$$

where ϕ_2^{s} is the fugacity coefficient of pure solid at T and P_2^{sat}. The exponential term is the Poynting correction for the fugacity of the pure solid, f_2^s. As $\phi_2^{s} \left(= f_2^s/P_2^{sat}\right)$ is always near unity due to the low vapor pressure of solids and the Poynting correction hardly ever has a value more than 2 or 3 and frequently much less (ref. 9), the most significant quantity of eqn. (10) is $\hat{\phi}_2$ which can be calculated from eqn. (7) and a simple cubic equation of state of the van der Waals type

$$P = \frac{RT}{v - b} - \frac{a(T)}{v^2 + ubv + wb^2} \tag{11}$$

For the PR equation, u = 2 and w = -1 in eqn. (11). The pure component parameters a and b for all simple cubic equations can be expressed in terms of the critical temperature and pressure of the pure substance. For the PR equation

$$a = \left(0.45724 \, R^2 T_c^2/P_c\right) . \, \alpha \tag{12}$$

and

$$b = 0.07780 \, RT_c/P_c \tag{13}$$

Hence, in the application of an equation of state to the representation of solubility data, it is essential to know the critical properties. Furthermore, in the current applications of equations of state for property calculations, the quantity α is taken to be temperature dependent and is determined from pure component vapor pressures. In phase equilibrium calculations, the quality of the calculated results depends very much on the capability of the equation of state to reproduce the vapor pressures. Therefore, the frequently adopted approach of expressing α in a generalized form should be avoided as much as practical, since a one percent deviation in α may cause a ten percent deviation in the vapor pressure calculation (ref. 10). In solid-fluid phase equilibrium calculations, difficulties are encountered because vapor pressures of the relatively nonvolatile solids are not always available. The α values determined from vapor pressures of saturated liquids are generally not suitable for extrapolating to the sublimation curve, nor are they suitable for the solvent in the supercritical region. In the calculation of mixture properties the conventional mixing rules frequently used are

$$a = \sum_i \sum_j y_i \, y_j \, a_{ij} \tag{14}$$

$$b = \sum_i y_i \, b_i \tag{15}$$

and the combining rule for a_{ij} is given by

$$a_{ij} = \left(a_{ii} \, a_{jj}\right)^{1/2} \left(1 - k_{ij}\right) \tag{16}$$

where a_{ii} and b_i are the pure component parameters and k_{ij} is an adjustable binary interaction parameter which in general must be determined from experimental data. It cannot be over-emphasized that proper selection of mixing rules for the determination of mixture parameters is very important in phase equilibrium calculations, especially for SCF solutions which are often highly asymmetric in nature. A number of mixing rules which are more complex than eqns. (14) - (16) and based on the concept of local compositions are available in the literature for further evaluation. With proper determination of α and selection of mixing rules, there is evidence in the literature (ref. 11, 12) that practically identical results in phase equilibrium calculations can be obtained from various cubic equation of state. On the other hand, the situation is quite different for density calculations, which very much depend on the form of the equations of state and on the number of temperature-dependent parameters in the equations, and are important in the treatment of supercritical solutions. Equations developed for asymmetric mixtures, for polar-nonpolar and polar-polar mixtures, as well as testing of various mixing rules have been reported in the literature (e.g. ref. 13-15). The applicability of these equations and mixing rules to the modelling of supercritical solutions needs testing and evaluation. Johnston et al. (ref. 16) recently reviewed method for correlating the solubility of a solid in pure and mixed supercritical solutions, and stated that enormous challenges remains to make equation of state models predictive. In spite of the possible difficult encountered, equations of state models can be used for extrapolations purposes once a good representation of solubility data is achieved.

To verify the influence of $\hat{\phi}_2$ on the enhancement of solubility of a solid in a SCF, it was calculated for the naphthalene (2) - ethylene (1) system using the solubility data of Tsekhanskaya et al. (ref. 3). The values of $\hat{\phi}_2$

obtained by means of the PR equation of state are found decreasing exponentially with pressure. For example, the $\widehat{\phi}_2$ value at 323 K and 220 bars has a value of 10^{-4}. As $\widehat{\phi}_2$ value are close to unity at very low pressures, an enhancement of solubility at these conditions is nearly 10^4 due to the nonideality of the SCF phase. In the calculation, the following two expressions were used for the calculation of α of eqn. (12).

$$\alpha_{C_2H_4} = \exp.\,[0.59704\,(1 - T_r)]$$

$$\alpha_{naph}^{1/2} = 1 + 1.1254\,(1 - T_r^{1/2}) - 0.1792\,(1 - T_r) - 2.3589 \times 10^{-3}\,(1 - T_r^2)$$

where $T_r\,(= T/T_c)$ is the reduced temperature. The sublimation pressure values reported by Fowler et al. (ref. 17) for naphthalene between 313 and 353 K were used to generate the α expression for naphthalene. The expression of α for ethylene followed that suggested by Adachi and Lu (ref. 18). As ethylene is in the supercritical state, the coefficient of the expression was determined not from vapor pressure data but from a regression of the PVT data (ref. 19). It should be mentioned that the solubility of naphthalene in ethylene is one of the few cases that can be represented by a number of simple cubic equations of state (ref. 11).

Solubility behaviour near the critical end points

The pressure dependence of $\widehat{\phi}_2$ is primarily responsible for the variation of the solubility of solid with pressure and can be evaluated from

$$\left(\frac{\partial \ln \widehat{\phi}_2}{\partial P}\right)_{T,\,y} = \frac{\bar{v}_2}{RT} - \frac{1}{P} \tag{17}$$

Hence an alternative expression for eqn. (7) is given by

$$RT \ln \widehat{\phi}_2 = \int_0^P \left[\bar{v}_2 - \frac{RT}{P}\right] dp \tag{18}$$

In other words, $\widehat{\phi}_2$ can be evaluated from a pressure integral of $\bar{v}_2$. As $\bar{v}_2$ is extremely sensitive to pressure, its behaviour in the vicinity of LCED has been investigated. For example, Azevedo and Prausnitz (ref. 20) evaluated partial molar volumes at the infinite dilution region of naphthalene in SCF ethylene, $\bar{v}_2^\infty$, by means of the Redlich-Kwong (RK) equation of state (ref. 21). The RK equation is represented by $u = 1$ and $w = 0$ in eqn. (11). The results indicate that $\bar{v}_2^\infty$ may reach negative infinite in the vicinity of the LCEP (T = 283.9 K, P = 51.9 bar, ref. 22), which is very close to the critical point of ethylene (T_c = 282.4 K, P_c = 52.1 bar). In other words, the solubility is extremely sensitive to pressure at LCEP due to the sensitivity of $\bar{v}_2$ with pressure. This observation is of course in agreement with eqn. (3).

Gitterman and Procaccia (ref. 23) analyzed the phenomenon of enhanced solubility of solids in SCF and showed that the slopes of solubility curves diverge near both the LCEP and UCEP. As both points are the intersections between the three-phase coexistence and the liquid-vapor critical curves, they are also points on the liquid-vapor critical curves. Since $\left(\partial \mu_2^g / \partial y_2\right)_{T,P}$ vanishes along these curves, the denominator of eqn. (3) vanishes at these two points. As $\left(\partial \mu_2^g / \partial y_2\right)_{T,P} \to 0$ upon approaching these two points, the slopes of the solubility curves $\left(\partial y_2 / \partial P\right)_T$ increase drastically, hence increase the solubility itself. A similar consideration may be applied to the variation of temperature at constant pressure with the same conclusions. Namely, the slope of the solubility curves $\left(\partial y_2 / \partial T\right)_p$ increase drastically in the vicinity of the LCEP and UCEP. It is this sensitivity of the solubility with small changes in pressure or temperature that provides the opportunity for SFE processes. At the LCEP, the amount of solid in the SCF solution is quite low even though there is a large enhancement of solubility. It is for this reason the location of the UCEP which occurs at relatively high pressure plays a more important role in the selection of operating conditions for SFE processes.

Density dependence of E

An alternative approach is to correlate the enhancement factor E in terms of density. Rowlinson and Richardson (ref. 24) used the virial equation of the Leiden form,

$$\frac{Pv}{RT} = 1 + \frac{B}{v} + \frac{C}{v^2} + \frac{D}{v^3} + \dots \tag{19}$$

where B, C etc. are the temperature and composition dependent virial coefficients, and developed the following expression for E

$$\ln E = \frac{v_2^s - 2B_{12}}{v} + \frac{v_2^s B_{11} - \frac{3}{2}C_{112}}{v^2} + \frac{v_2^s C_{111} - \frac{4}{3}D_{1112}}{v^3} + \dots \tag{20}$$
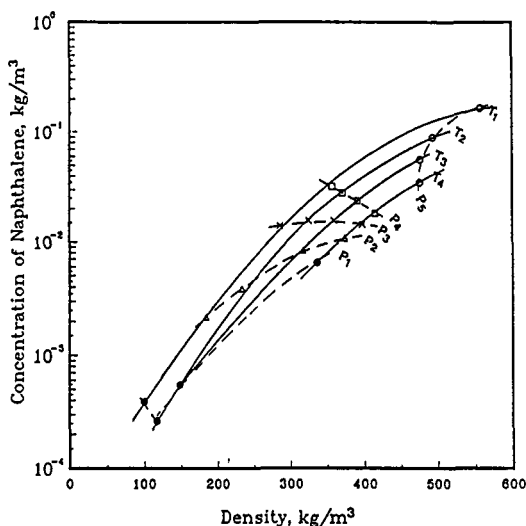
Fig. 3.   Solubility of naphthalene in ethylene
(ref. 3) as a function of density

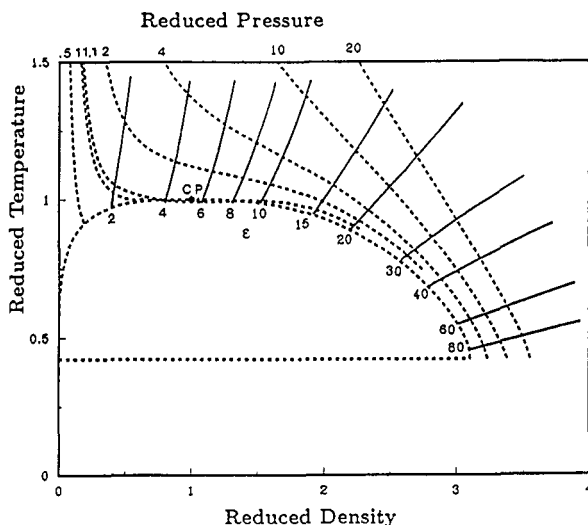|	
$T_1 = 285$ K	$T_2 = 298$ K
$T_3 = 308$ K	$T_4 = 318$ K
$P_1 = 61$ bar	$P_2 = 81$ bar
$P_3 = 101$ bar	$P_4 = 127$ bar
$P_5 = 304$ bar	

Fig. 4.   Reduced temperature vs. reduced
density diagram for water with constant
dielectric constant ε lines (solid lines).
CP - critical point.

for the simple case discussed above, namely, the solubility of a solid in a SCF. In eqn. (20), B_{11} and C_{111} are the virial coefficients of the pure SCF solvent, and B_{12}, C_{112}, D_{1112} are the cross-virial coefficients. All of these coefficients are independent of pressure. Consequently, an isothermal compression would decrease the molar volume v and hence increase E and the solubility. The decrease in v is equivalent to the increase in density ρ. The solubility of naphthalene in supercritical ethylene (ref. 3) is depicted in Fig. 3 as a function of density at four different temperatures to demonstrate the simple trend of dependence.

There are several simple expressions available in the literature for calculating concentration of solute in supercritical fluids with density or density-dependent properties (e.g. ref. 11). Johnston et al. (ref. 16) suggested that simple empirical correlation of E versus density be used if the goal is to correlate solubility isotherms.

SELECTION OF SUPERCRITICAL SOLVENTS

Williams (25) truncated eqn. (20) to the first term on the right-hand side and considered the factor E with a correlation of the second virial coefficient for non polar gases. He concluded that at a given temperature, gases of high T_c having large negative values of B_{12}, the cross-virial coefficient which represents interaction between the molecules of the gas and the solute, are better solvents than those of low T_c. For example ethylene ($T_c = 282.4$ K), ethane ($T_c = 305.4$ K) and carbon dioxide ($T_c = 304.2$ K) are better solvents than nitrogen ($T_c = 126.2$ K) and methane($T_c = 190.6$ K) for phenanthrene. In practical application, carbon dioxide is one of the most selected solvents, because it is non-flammable, non-corrosive, relatively inexpensive and readily available in high purity. It is particularly suitable for food and pharmaceutical processing because it introduces no health hazards. In addition to ethylene and ethane, SCF solvents studied in the literature include xenon (a less polar/polarizable solvent than carbon dioxide at similar reduced densities, ref. 26), toluene (an aromatic with a high critical temperature of 591.7 K, suitable for coal processing, ref. 25), ammonia (a polar solvent with a critical temperature of 405.6 K, suitable for extracting polar organic molecules, ref. 27) and water (a solvent with its dielectric constant drastically changed in its supercritical states, ref. 28).

Among the solvent properties, such as solubility parameters, dielectric constant, dipole moment, hydrogen bonding and acidity or basicity, dielectric constant ε tends to be the frequently used guide to solvent suitability. Evidence indicates that pure compounds have a tendency to dissolve to advantage in the solvent having a similar dielectric constant. It is for this reason that water in the supercritical state becomes a good solvent for organic materials and gases, leading to the destruction of aqueous waste (ref. 29). Normal liquid water at 298 K and 1 bar has an ε value of 78.46. The ε value decreases rapidly with increasing temperature along the saturation curve, and reduces to 5 at the critical point ($T_c = 647.3$ K and $P_c = 220.5$ bar). The variation of ε of water with temperature and density at constant pressures (ref. 28) are plotted in Fig. 4 in terms of reduced temperature, pressure and density. The constant ε values are shown in solid lines. In the vicinity of the critical temperature ($T_r = 1$), a drastic variation of density, and hence ε, accompanies a small change in temperature making supercritical water a suitable solvent for a variety of organic substances.

EFFECTS OF ENTRAINERS

The selection of appropriate entrainers (cosolvents) to enhance the solubility of the desired solute is essential in SFE operations. For many systems, the increase in solvent power of SCF when a cosolvent is added is due to an increase in the density of the solvent mixture. This increased solubility is comparable to that which can be achieved with the pure solvent through the variation of T and P. But the dramatic enhancement of solubility due to the addition of a cosolvent which cannot be obtained by the variation of density is due to the chemical interaction between the solute and the cosolvent. It is known that solubility may increase by a factor of 3 to 7 by the addition of a small amount of polar solvent for systems that form strong hydrogen bonds (ref. 30). The polar cosolvents frequently used includes methanol and acetone.

Walsh et al. (ref. 31) studied the experimental results reported by Van Alsten et al. (ref. 32) and Schmitt and Reid (ref. 33) and showed that the entrainer effect was caused by a chemical association between the cosolvent and the solute.

Van Alsten et al. (ref. 32) studied the solubility of phenanthrene, florene, fluorenone, dibenzofuran and acridine in pure carbon dioxide and in a mixed solvent of 95 mol % carbon dioxide and 5 mol % methanol. These five solids are similar in size and structure but with singular difference in chemical functional group. Only the solubility of acridine was enhanced in the mixed solvent. Walsh et al. (ref. 31) further noted that the trend in solubility enhancement does not follow the trend in polarity for these mixtures as the dipole moment of fluorence is greater than that of acridine but the solubility enhancement of fluorenone is negligible compared to that of acridine. The infrared spectrograph showed a complex between acridine and methanol but not between the other four solutes and methanol.

Schmitt and Reid (ref. 33) measured the solubility of phenanthrene and benzoic acid in either supercritical carbon dioxide or ethane using benzene, cyclohexane, acetone or methylene chloride as a cosolvent. They observed significant solubility enhancement for the system benzoic acid - ethane - acetone but not for any other systems investigated. The infrared spectrograph also showed a complex between benzoic acid and acetone but not for other solute-cosolvent mixtures. The cosolvent acetone served as an entrainer for benzoic acid in supercritical ethane but not in supercritical carbon dioxide indicates the importance on the selection of the supercritical solvent. Walsh et al. (ref. 31) considered the chemical function groups of carbon dioxide which has two carbonyl oxygens that compete with other hydrogen bond acceptors for the hydrogen bond donors, and the relative concentration of carbon dioxide and the cosolvent. A cosolvent may also play a role on the selectivity for a component in a mixture of solutes (e.g. ref. 34).

FURTHER REMARKS ON MODELLING SUPERCRITICAL MIXTURES

Recent efforts made in the literature for overcoming the difficulties encountered in modelling supercritical mixtures by means of the equations of state approach include the replacement of the repulsive term of eqn. (3) with an accurate expression for hard spheres, and the modification of mixing rules with the binary interaction parameters taken to be temperature, pressure, density and/or composition dependent. A recent review on these subjects is available (ref. 16).

More recently, Kato et al. (ref. 35) correlated solid-supercritical fluid equilibria using their pseudo-cubic equation of state (ref. 36).

$$P = \frac{RT}{v^* - b} - \frac{a}{v^{*2}} \tag{21}$$

$$v^* = \frac{(v - \varepsilon b)(v + \sigma b)}{v} \tag{22}$$

where $\varepsilon = (1 - \theta)(\xi - 2)$, $\sigma = (1 - \theta)(\xi + 2)$, and $\xi = \sqrt{\frac{(4 - \theta)}{(1 - \theta)}}$. The following empirical mixing rules were used in the calculation:

$$a = \sum_i \sum_j y_i y_j a_{ij}, \qquad a_{ij} = (1 - k_{ij}) \cdot \sqrt{a_i a_j}$$

$$b = \sum_i y_i b_i \tag{23}$$

$$\theta = \sum_i \sum_j y_i y_j \theta_{ij}, \qquad \theta_{ij} = (1 - c_{ij}) \cdot \sqrt{\theta_i \theta_j}$$

The correlated results using the data of Johnston et al. (ref. 37) for the solubility of anthracene in ethane at 323 K are illustrated in Fig. 5. The calculated average of $[|y_{calc.} - y_{expt}| / y_{expt}]$ is 0.051, which is considered very satisfactory.

An attempt was made in this study to correlate supercritical mixture properties including vapor compositions and density of the three-component supercritical phase by means of a simple cubic equation. The volume-translated PR equation proposed by Yu and Lu (ref. 13)

$$P = \frac{RT}{v - b} - \frac{a(T)}{v^2 + (2b - 4c)v + (2c^2 - b^2)} \tag{24}$$

was modified (ref. 10) and adopted for the calculation. Although eqn. (24) appears to be a three-parameter
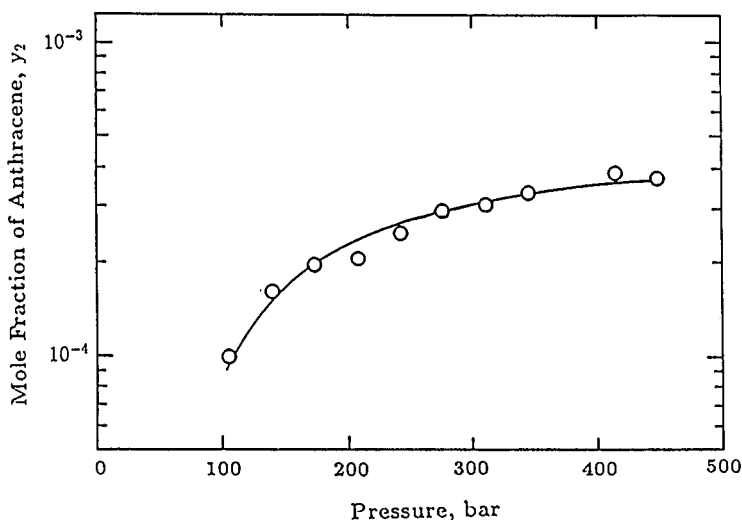
Fig. 5. Comparison of calculated and experimental solubilities of anthracene in ethane at 323.15 K. O, experimental data (ref. 36); ---- calculated, pseudo-cubic equation.

equation, only two of them are independent. It can be shown that both b and c are related to u of eqn. (3) and that $c/b = (2-u)/4$ and $b = 0.3112\ RT_c/[(2 + u)\ P_c]$. The experimental data reported by Dobbs et al. (ref. 30) for the system benzoic acid (2) - carbon dioxide (1) - methanol (3) at 308 K was used for the correlation. In the experiments, the supercritical solvent carbon dioxide was doped with 3.5 mol % methanol. The α and u values used in the calculation for benzoic acid and carbon dioxide are given by

Benzoic acid $\qquad \alpha = \left[1 + 1.6249\!\left(1 - T_r^{1/2}\right)\right]^2$

$$u = 2.2$$

Carbon dioxide $\qquad \alpha = \exp[0.5856(1-T_r)]$

$$u = 1.65246$$

The α and u values reported previously (ref. 10) for methanol were adopted. The mixing rules adopted in the calculation are given by

$$a = \sum_i \sum_j y_i y_j\, a_{ij}, \quad a_{ij} = \left(a_{ii}\, a_{jj}\right)^{1/2} \left[1 - k_{ij} - l_{ij}\left(y_i - y_j\right)\right] \tag{25}$$

$$b = \sum_i \sum_j y_i y_j\, b_{ij}, \quad b_{ij} = \left(b_{ii} + b_{jj}\right)\left(1 - m_{ij}\right)/2 \tag{26}$$

$$c = \sum_i \sum_j y_i y_j\, c_{ij}, \quad c_{ij} = \left(c_{ii} + c_{jj}\right)\left(1 - m_{ij}\right)/2 \tag{27}$$

In eqn. (25), the mixing rule for a_{ij} follows that proposed by Adachi and Sugie (ref. 38) and k_{ij} (=k_{ji}) and l_{ij}(=-l_{ji}) are the binary interaction coefficients. In eqns. (26) and (27), m_{ij} is the binary interaction coefficient accounting for the differences in molecular sizes. The binary interaction parameters for the three constituent binaries are obtained in the following manner. The solubility data of benzoic acid (2) in carbon dioxide (1) at 308 K (ref. 30) were correlated with $l_{12} = 0$ so that the volumetric contribution in the mixing rule is emphasized. For the binary system carbon dioxide (1) - methanol (3), the data available at 298 K (ref. 39) were correlated with $m_{13} = 0$ to place emphasis on the composition contribution in the mixing rule. As no data are available for the binary system benzoic acid (2) - methanol (3), the binary interaction parameters for this system were obtained from the ternary data (ref. 30) together with the binary interaction parameters for the other two binaries. The values of the binary interaction parameters thus obtained are as follows:

$k_{12} = -0.0269 \qquad\qquad l_{12} = 0 \qquad\qquad m_{12} = -0.291$

$k_{13} = 0.0506 \qquad\qquad l_{13} = 0.0123 \qquad\qquad m_{13} = 0$

$k_{23} = -0.5930 \qquad\qquad l_{23} = -0.5386 \qquad\qquad m_{23} = -0.3787$

The average absolute percent deviations in the calculated y_2 and molar volume for the ternary mixtures are 1.95 and 1.33 respectively. The agreement obtained between the calculated and experimental values is depicted in Figs. 6 and 7. These deviations are considered very satisfactory. Even though the parameters were obtained from data fitting, these values may be applied to the same system with different amount of the cosolvent.
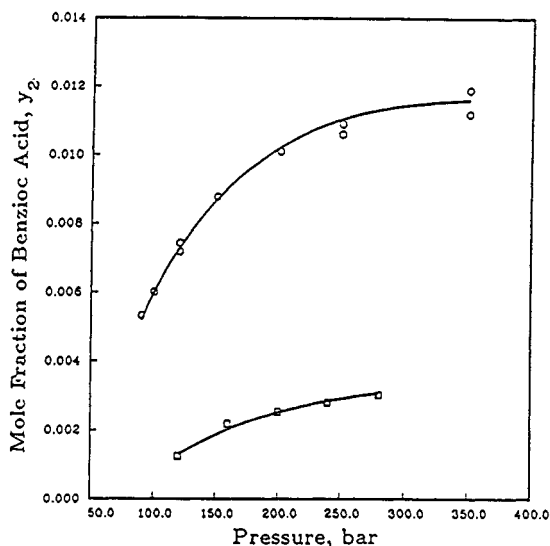
Acknowledgement

Fig. 6. Comparison of calculated and experimental mole fractions of benzoic acid in supercritical carbon dioxide at 308 K (ref. 30).□, without cosolvent;○, with cosolvent methanol.
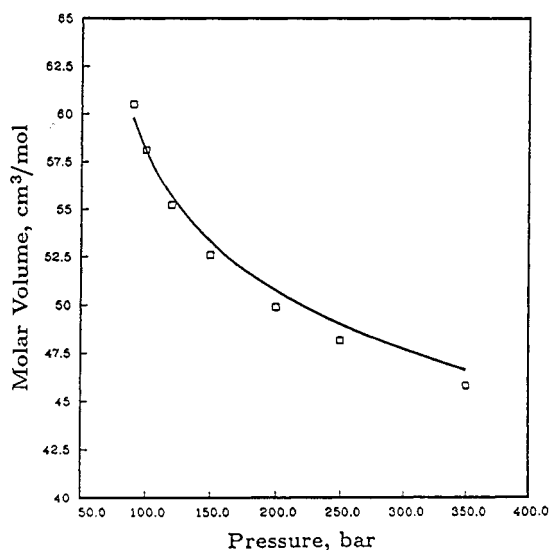
Fig. 7. Comparison of calculated and experimental molar volumes of benzoic acid - carbon dioxide - methanol at 309 K. The supercritical solvent carbon dioxide was doped with 3.5 mole % methanol.

REFERENCES

1. J.B. Hannay and J. Hogarth, Proc. Roy. Soc. (London), A29 324-326 (1879).
2. B.C.-Y. Lu and D. Zhang, Pure Appl. Chem., 61 1065-1074 (1989).
3. Yu, V. Tsekhanskaya, M.B. Tomter and E.V. Mushkina, Russ. J. Phys. Chem. 38 1173-1176 (1964).
4. RB. Hinckley and R.C. Reid, AIChE Journal 10 416-417 (1964).
5. J.J. Czubryt, M.N. Myers and J.C. Giddings, J. Phys. Chem., 74 4260-4266 (1970).
6. K. Denbigh, The Principles of Chemical Equilibrium Cambridge University Press, London (1955).
7. R.T. Kurnik and R.C. Reid, AIChE Journal, 27 861-863 (1981).
8. D.Y. Peng and D.B. Robinson, Ind. Eng. Chem. Fund., 15 59-64 (1976).
9. J.M. Prausnitz, Molecular Thermodynamics of Fluid Phase Equilibria Prentice-Hall, Englewood Cliffs, NJ (1969).
10. W. Sheng and B.C.-Y. Lu, Fluid Phase Equilib., 56 71-80 (1990).
11. Y. Adachi and B.C.-Y. Lu, Fluid Phase Equilib. 14 147-156 (1983).
12. Y. Adachi and B.C.-Y. Lu, Can. J. Chem. Eng., 63 497-503 (1985).
13. J.-M. Yu and B.C.-Y. Lu, Fluid Phase Equilib., 34 1-19 (1987).
14. M.R. Margerum, H. Sugie and B.C.-Y. Lu, Chem. Eng. Comm., 92 153-167 (1990).
15. M.R. Margerum and B.C.-Y. Lu, Fluid Phase Equilib., 56 105-118 (1990).
16. K.P. Johnson, D.G. Peck and S. Kim, Ind. Eng. Chem. Res., 28 1115-1125 (1989).
17. L. Fowler, W.N. Trump and C.E. Vogler, J. Chem. Eng. Data, 13 209-210 (1968).
18. Y. Adachi and B.C.-Y. Lu, AIChE Journal, 30 991-993 (1984).
19. S. Angus, B. Armstrong and K.M. de Reuck, International Thermodynamic Tables of Fluid State. Ethylene, Butterworths, London (1974).
20. E.G. Azevedo and J.M. Prausnitz, Chempor '85, 19/1 - 19/6, Coimbra, Portugal, April 15-19 (1985).
21. O. Redlich and J.N.S. Kwong, Chem. Rev., 44 233-244 (1949).
22. C.A. van Gunst, F.E.C. Scheffer and G.A.M. Diepen, J. Phys. Chem., 57 578-581 (1953).
23. M. Gitterman and I. Procaccia, J. Chem. Phys., 78 2648-2654 (1983).
24. J.S. Rowlinson and M.J. Richardson, Adv. Chem. Phys., 2 85-118 (1959).
25. D.F. Williams, Chem. Eng. Sci., 36 1769-1788 (1981).
26. R.D. Smith, S.L. Frye, C.R. Yonker and R.W. Gale, J. Phys. Chem., 91 3059-3062 (1987).
27. C.R. Yonker and R.D. Smith, Fluid Phase Equilib., 22 175-183 (1985).
28. M. Uematsu and E.U. Franck, J. Phys. Chem. Reference Data, 9 1291-1306 (1980).
29. T.B. Thomason and M. Modell, Hazardous Waste, 1 453-467 (1984).
30. J.M. Dobbs, J.M. Wong, R.J. Lahiere and K.P. Johnson, Ind. Eng. Chem. Res., 26 56-65 (1987).
31. J.M. Walsh, G.D. Ikonomou and M.D. Donohue, Fluid Phase Equilib., 33 295-304 (1987).
32. J.G. Van Alsten, P.C. Hansen and C.A. Eckert, presented at the AIChE annual meeting, Paper 84a, San Francisco (1984).
33. W.J. Schmitt and R.C. Reid, Fluid Phase Equilib., 32 77-99 (1986).
34. J.M. Dobbs and K.P. Johnston, Ind. Eng. Chem. Res., 26 1476-1482 (1987).
35. M. Kato, M. Yamaguchi and T. Muramatsu, presented at CHISA 90, Session C8, Prague, Czechoslovakia, 1990.
36. M. Kato and H. Tanaka, Adv. Cryo. Eng., 31 1169-1179 (1986).
37. K.P. Johnston, D.H. Ziger, C.A. Eckert, Ind. Eng. Chem. Fundam., 21, 191-197 (1982).
38. Y. Adachi and H. Sugie, Fluid Phase Equilib., 28 103-118 (1986).
39. T. Katayama, K. Ohgaki, G. Maekawa, M.Goto and T. Nagano, J. Chem. Eng. Jpn., 8 89-92 (1975).